International Journal of Application or Innovation in Engineering & Management (IJAIEM)
Web Site: www.ijaiem.org Email: editor@ijaiem.org
Volume 4, Issue 6, June 2015 **ISSN 2319 - 4847**

A stereolithography-based 3D-printed torsional mirror scanner actuated by vertical comb-drive

Jun Mizuno[1], Takashi Kakizaki[2], Satoshi Takahashi[3] , Subaru Kudo[4]

[1] Ishinomaki Senshu University, Department of Mechanical Engineering
1 Shinmito, Minamisakai, Ishinomaki City, Miyagi Prefecture, Japan

[2] Ishinomaki Senshu University, Department of Mechanical System Engineering
1 Shinmito, Minamisakai, Ishinomaki City, Miyagi Prefecture, Japan

[3] Ishinomaki Senshu University, Department of Mechanical Engineering
1 Shinmito, Minamisakai, Ishinomaki City, Miyagi Prefecture, Japan

[4]Ishinomaki Senshu University, Department of Information Technology and Electronics
1 Shinmito, Minamisakai, Ishinomaki City, Miyagi Prefecture, Japan

ABSTRACT

We have designed, fabricated and characterized a torsional mirror scanner which is electrostatically actuated by vertical comb-drive electrodes. As in the previous works of the authors, such a 3D-printed device, which performs an electromechanical function, has been named as SMEMS (Sub-Milli Electro-Mechanical Systems) device. Up to now, SMEMS devices have been fabricated by a plaster-based 3D-printer. In this work, we have fabricated for the first time a SMEMS device by a stereolithography-based 3D-printer. The scanner consists of a reflector plate with dimensions of (9 x 7) mm and 1mm in thickness, which is supported on both sides of the plate end faces by (1 x 1) mm beam-shaped hinge. The gap between the stationary and movable comb-drive electrodes is 1mm. Since the scanner design has not been optimized for large deflecting angle, we have obtained a small optically full-width deflection angle of 1.1' (minute) at the resonance frequency of 99Hz. Tough the deflection angle was small, it has been enough to demonstrate that the scanner electromechanically actuates a rotational motion.

Keywords: mirror scanner, 3D-printer, SMEMS, stereolithography

1. INTRODUCTION

Advances on 3D-CAD (Computer Aided Design), CAE (Computer Aided Engineering) and CAM (Computer Aided Manufacturing) [1]–[3] brought an innovative fabrication technology – the 3D-printing technology – in the world. In recent years, several 3D-printers have been developed and sold in the rapid prototyping market [4]. Recently, the authors have demonstrated that devices fabricated by 3D-printers can perform electromechanical functions once actuator design is appropriately conducted, and electrodes are formed on the device surface by suitably masking and metallizing thereafter [5], [6]. These devices have been named by the authors as SMEMS (Sub-Milli Electro-Mechanical Systems) devices. This original concept is based on hybridly merging the 3D-printing fabrication and MEMS (Micro Electro-Mechanical Systems) design method. In the fabrication point of view, MEMS uses GHG (greenhouse gases) such as SF_6 (sulfur hexafluoride) and C_4F_8 (perfluorocyclobutane) gases for key fabrication processes for Bosh-based etching [7] and massive volume of CO_2 gas for supercritical dry [8] which have been established for more than a decade. On the other hand, SMEMS do not use any hazardous chemicals or gases. Thus, it is greatly expected as an environmental-clean fabrication technology, in despite of the 3D printing method.

Up to now, the authors have demonstrated the feasibility of electro-mechanical actuation of SMEMS devices fabricated by plaster-based printers [5], [6], [9] – [11]. In this work, a SMEMS device has been fabricated by a stereolithography-based 3D-printer for the first time. The stereolithography-based 3D-printer uses ultraviolet (UV) curing resin as a structure material. In the case of plaster-based printer, plaster material is used. Compared to fragile properties of plasters, flexible properties of UV curing resins are mostly desired for using in device structures, in particular for spring parts which allow the structure to move.

In this paper, design, fabrication and characterization of a SMEMS torsional mirror scanner fabricated by a stereolithography-based 3D-printers is described. We have demonstrated that the device can perform a rotationally electro-mechanical actuation. Vertical comb-drive electrodes have been adopted for the device actuator.

2. DESIGN

2.13D-CAD design

The SMEMS torsional mirror scanner has been designed by a 3D-CAD tool, as shown in Fig. 1. The comb-drive actuator consists of interdigitated comb fingers which are placed mutually in different layers. This type of structure is called vertical comb-drives. Such a structure is clearly seen in Fig. 2, which shows the cross sectional view at the plane parallel to the comb-drive actuators. In order to assist the understanding of the mirror scanner design, we have split up the device in two parts, the stationary and movable parts, as shown in Fig. 3.

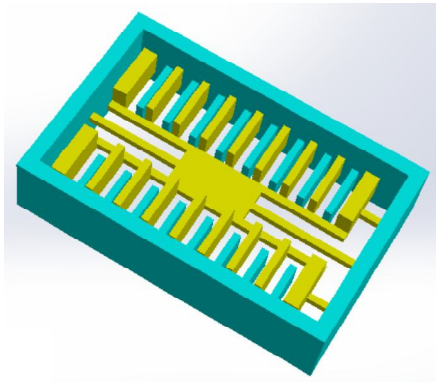

Figure 1 SMEMS mirror scanner designed by a 3D-CAD

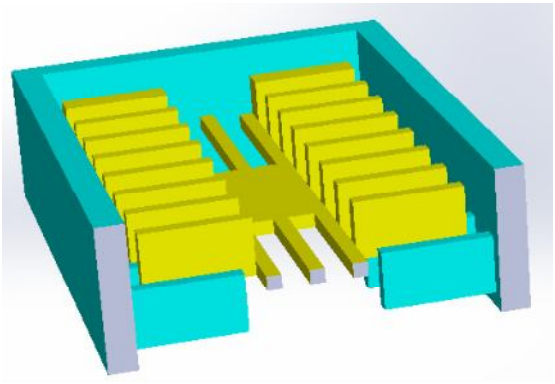

Figure 2 Cross sectional view

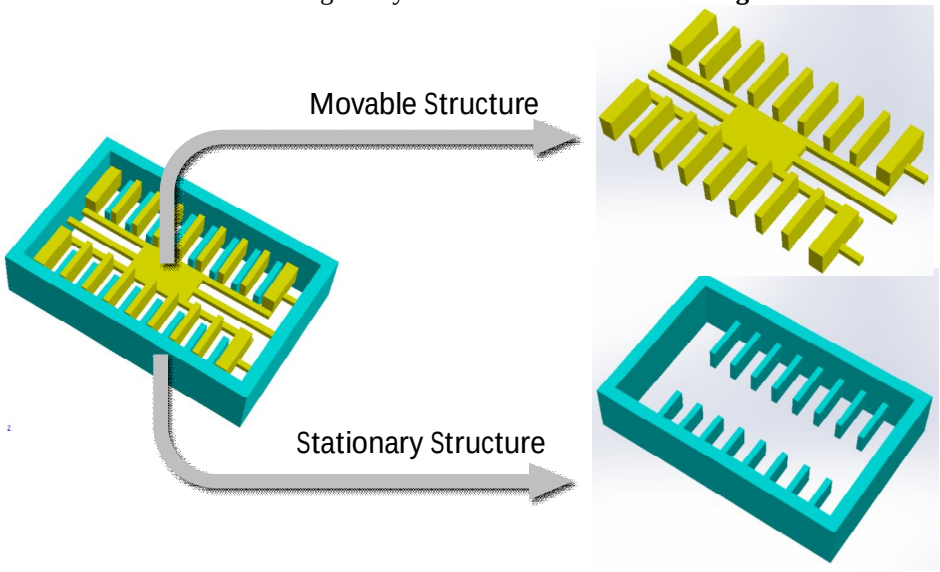

Figure 3 3D-CAD data split up into movable and stationary structures

The stationary part consists of a surrounding frame and eight comb fingers coming out from each inner side of the frame. The frame dimensions are as follows: outer size of (28 x 43) mm and 10mm in thickness. The frame rim is 2mm. The comb finger dimensions are as follows: 1mm in width, 7.5mm in length and 1mm in thickness. The depth between the top surface of the frame and the comb finger is 5 mm.

The movable part consists of five components: 1) a central rectangular plate for reflecting the incoming laser beam (reflector plate, as follows); 2) two torsional beam-shaped hinges that are used as torsional springs for realizing a rotational motion and also for supporting the overall movable structure. These beams come out from both center side of the reflector plate and its end faces are merged with the inner lateral surface of the frame; 3) four support beams coming out from the four corners of the reflector plate for supporting the comb fingers; 4) nine comb fingers coming out from both outer side of the support beams (including also the outer side of the reflector plate); and finally 5) four protuberances (auxiliary beams, as follows) coming out from the outer side of each four comb fingers located nearest the frame. These auxiliary beams are necessary so that the movable structure does not drop during the fabrication process. At the end of the fabrication, they are removed by an ultrasonic cutter in order to release the movable structure. The reflector plate dimensions are as follow: outer size of (6.7 x 11) mm and 1mm in thickness. The torsional beam-shaped hinge is 1mm in width, 15mm in length and 1mm in thickness. Both torsional hinges should have a same length. However the other one is 2mm shorter caused by a small miss during the CAD design. The length difference of

the auxiliary beams is also 2mm and as a result, the reflector plate and frame are not exactly centered. Tough, this factor would not affect the overall performance of the mirror scanner. The support beam is 1mm in width, 12mm in length and 1mm in thickness. The comb finger dimensions are similar to that of the stationary ones. Only the four comb fingers located at the corner nearest the inner lateral surface of the frame are 1mm thicker. The reason is to avoid bending problems because during the actuation, electrostatic force acts at only one side for these four fingers. The depth between the top surface of the frame and the comb finger is 2 mm.
The gap between the movable and stationary comb fingers is 1mm and their overlap in the vertical direction is 1mm. This overlap is very important to reduce the drive voltage as described below.

2.2Drive principle

The drive principle is based on differential voltage drive method described by the authors elsewhere [11]. The stationary comb fingers on the right and on the left are electrically isolated (see Fig 2). The movable comb fingers are grounded. An electrostatic force, which is induced by applying a voltage on one side of the stationary fingers, pulls the movable comb finger side toward the stationary one. The overall movable structure would move vertically down. However, since this structure is constrained by the torsional hinges, it will rotate around this hinge axis. The mirror scanner would rotate consecutively in clockwise and counterclockwise direction, if a voltage is alternately applied to the left and to the right comb fingers. In concrete terms, both (right and left) stationary comb fingers are electrically connected to a sinusoidal voltage source with a maximum amplitude V_{ac} peak-to-peak (V_{ac}, as follows) and positively biased at a DC voltage source with a value of $V_{bias} = V_{ac}$ /2. To realize a differential voltage driving, the applied voltages on right and left comb fingers are mutually inverted (i.e., 180 degrees shifted). Thus, if the maximum sinusoidal voltage is applied to one of the finger combs (for example, right ones), the left comb fingers are at zero volt and vice versa.

3.FABRICATION

For the fabrication, we used the stereolithography-based 3D-printer (MiiCraft™). The fabrication process is described as following. Once the 3D-CAD design of the SMEMS mirror scanner is completed, its data is converted to standard triangulated language (STL, as follows) format and downloaded on the B9Creator™ software for adding supports beneath the device surface. This process is inevitable for stereolithography-based 3D-printers. The device shape is greatly dependent on the number of support and its shape. Thus, if the support design is not well conducted, deformation of the device would occur during the fabrication. We have tested several support conditions, and we have succeeded in reproduce the 3D-CAD data for post shaped supports that have the following dimensions: 1mm in diameter, 5mm in height, and separation distances between posts of at least 1mm to 2mm. The added supports on the device are shown in Fig. 4 (a) top side view, and (b) bottom side view. The hole structure is saved again in STL file and then sliced by using MiiCraft Suite™ software (slice thickness has been set at 100μm).

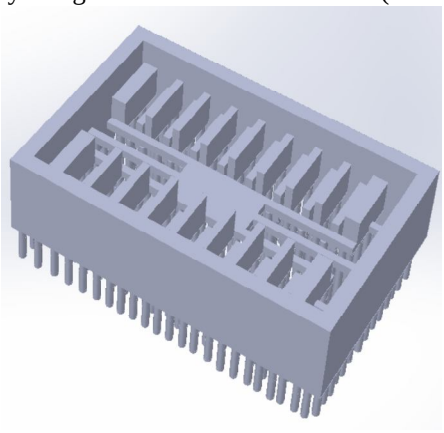

Figure 4 (a) Top side view of the data ready to be printed

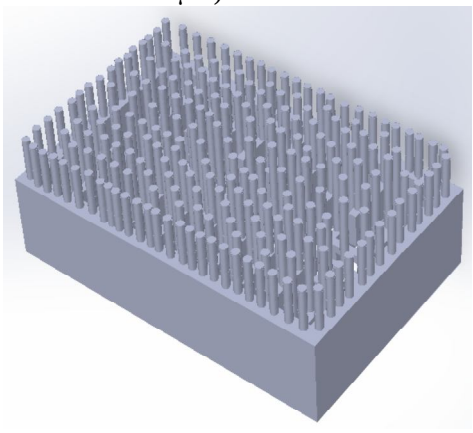

Figure 4 (b) Bottom side view (several support posts)

The fabrication starts from a thin planar layer (default) with a work size of the pedestal where the structure will be printed. Then, posts and device are sequentially printed layer by layer. After the last layer is finished, the fabricated device is transferred to another compartment of the 3D-printer for post curing process (10 minutes). Then, the device is removed from the pedestal and supports are removed by an ultrasonic cutter. The fabricated structure is shown in Fig. 5 (a) top side view, and (b) bottom side view, before cutting the supports. The device after cutting all supports is shown in Fig. 6 (a). However, the fabrication process is not finished yet. As described above, electrodes must be formed on the device surface for electro-mechanical actuation. The metallization is performed by an Au ion sputter. Before this step, a polyimide film is used for masking appropriate areas, in order to obtain electrical isolation between the stationary

comb-drive actuator parts and the ground. These films are removed after the metallization. The complete device is shown in Fig. 6 (b). Copper wires stuck by conductive tapes for applying drive voltages can be seen in this figure. Moreover, a thin Au coated glass piece is placed on the reflector plate in order to improve the laser beam reflection during the characterization. Fig. 7 shows the flowchart of the entire fabrication process as described above.

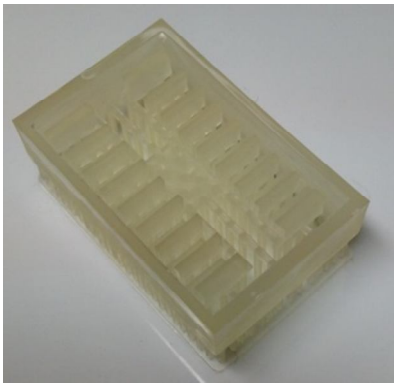

Figure 5 (a) The fabricated device

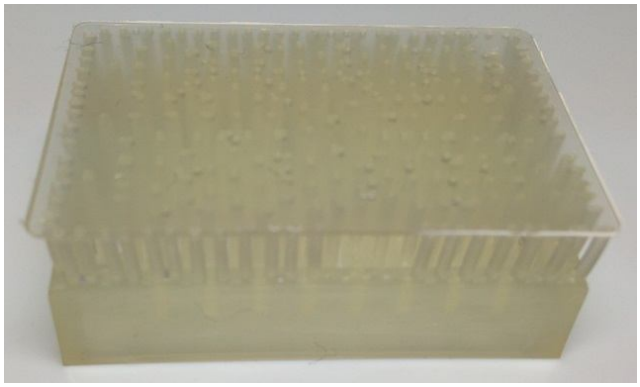

Figure 5 (b) Bottom side view (start layer and supports)

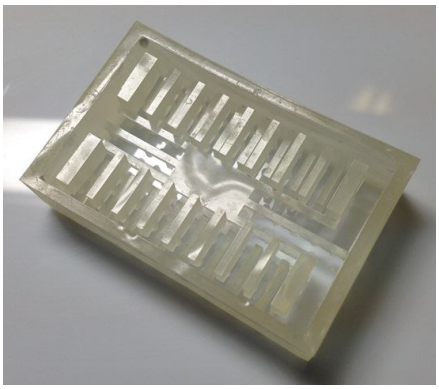

Figure 6 (a) Device after cutting supports

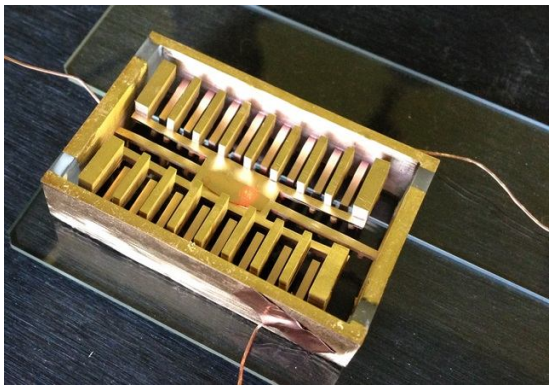

Figure 6 (b) Complete device (ready for characterization)

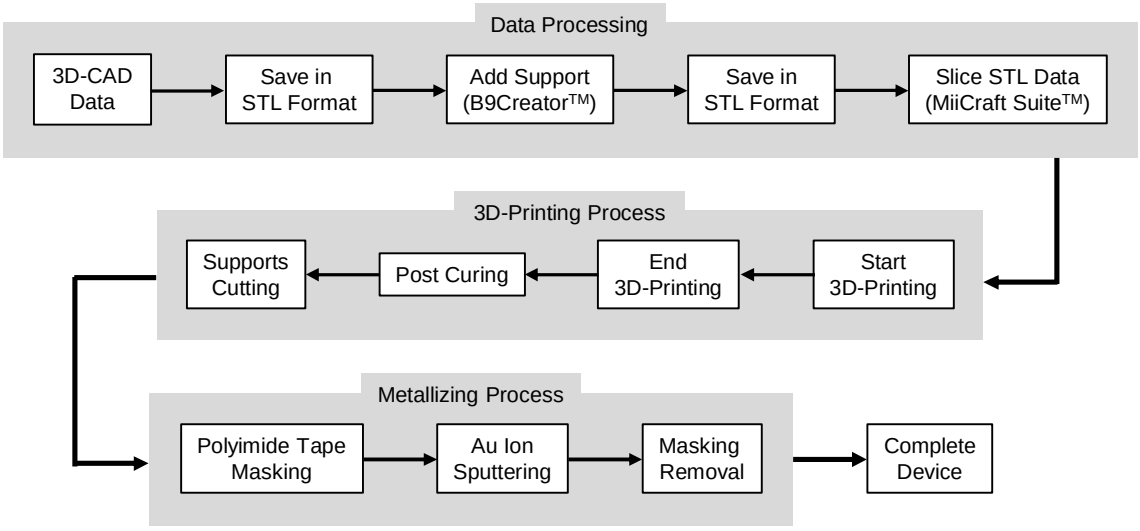

Figure 7 Flowchart of the fabrication process

4.CHARACTERIZATION

4.1 Experimental Setup

The fabricated device characterization is focused on the frequency response and consecutively the mechanical quality factor (Q-factor, as follows), and the dependence relation between the deflected angle and the applied voltage. The experimental setup is similar to that of described by the authors elsewhere [11].

This time, besides the laser-based optical setup by using a position sensor detector (PSD, as follows), we have also used

an autocollimator equipment for measuring the maximum deflected angle at the resonance frequency as shown in Fig 8 (a). Regarding the laser-based optical setup, an outgoing He-Ne laser beam is suitably steered by a set of steering mirrors to incident on the glass piece above the reflector plate at an angle of about 45 degrees. A PSD (C10443-02, Hamamatsu Photonics K. K.) is placed about 1m far away from the device and at a height of about 1m. Thus, the device and the PSD are trigonometrically located as shown in Fig.8 (b) where exact distances have been indicated on. The window sensor of the PSD is adjusted to be perpendicular to the beam direction. The PSD outputs a real-time voltage which is proportional to the incident beam position on the sensor, and its relation is 1volt per millimeter (1V/mm). Based on this relation and the trigonometric position of the device and the sensor, we can calculate the full-width optical deflected angle of the mirror scanner as described afterwards. The PSD output signal is collected by a digital storage oscilloscope (TDS2004C, Tektronix Corporation). The autocollimator (6D, Nikon Corporation) is placed above the device and it is adjusted so that the reflected light enters the visual field of the finder.

Regarding the drive voltage, sinusoidal differential voltages with amplitudes of 200 Vpp (Volts peak-to-peak) with a bias voltage of 100V are reproduced by a dual-channel function generator (WF1948, NF Corporation) and then amplified by a dual-channel signal amplifier (9200A, Tabor Electronics Ltd.). The function generator reproduces two sinusoidal signals that are mutually inverted with amplitudes of 4Vpp and offset by 2V. Then, these two signals are amplified by fifty times. These two signals are connected to each side of the comb-drive actuator. The signal amplifier also outputs 100x attenuated monitor signals which are connected to the same oscilloscope to that of connected to the PSD.

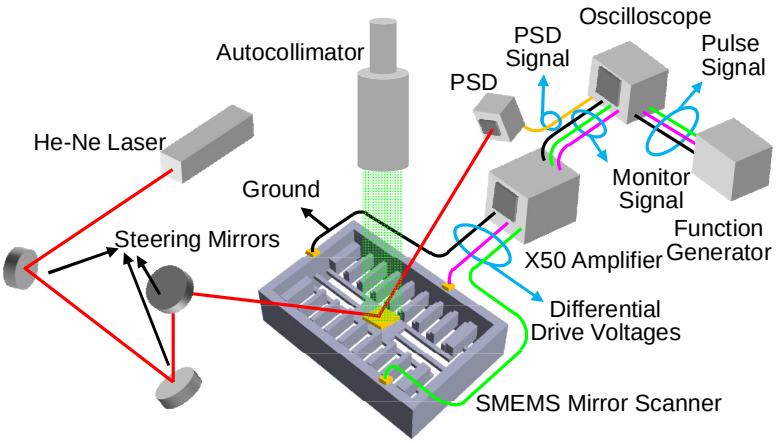

Figure 8 (a) Experimental measurement setup

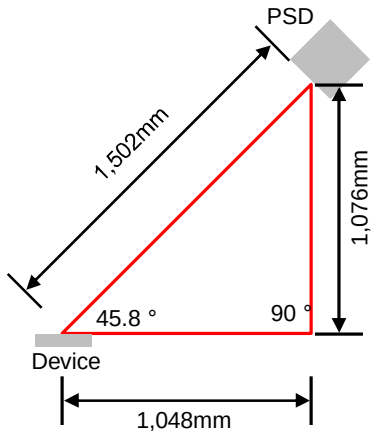

Figure 8 (b) Trigonometric relation (device x PSD)

4.2 Results and Discussion

Based on the experimental setup describe above, the frequency response of the fabricated mirror scanner has been measured as shown in Fig. 9. The peak obtained at 99Hz is the resonance frequency of this device. From this measurement the Q-factor has been estimated to be around 10. The frequency of the function generator has been manually swept and data of the frequency and PSD voltage have been collected as illustrated by points (the smooth line has been created automatically by Excel). Furthermore, the amplitude of the PSD voltage has been normalized, i.e. transforming values into a range of 0 and 1, by means of dividing the collected data by the voltage at resonance frequency (which is the maximum value). The differential drive voltages and the PSD output voltage have been plotted in Fig. 10 at the resonance operation. In this graph raw data collected from the oscilloscope have been plotted. The horizontal, left and right vertical axes are time, peak-to-peak differential drive voltages, and PSD voltage, respectively. An average peak-to-peak voltage of 0.448mV has been obtained at the resonance frequency. Thus, the calculated full-width scan length is 0.448mm, according to the relation between the PSD voltage and beam position as described in the previous subsection (1V/mm). Based on the trigonometric relation between the device and the PSD, and the full-width length, we have obtained an optically full width deflection angle of 1.12’ (minute). We have also measured this angle by the autocollimator. In this case, the mechanically deflection angle is directly measured. We have obtained a value of 34’’ (second) based on this method. Since the optical angle is twice the mechanical one, the previous value after doubled and converted to minute unit, we obtained a value of 1.13’ (minute). The value for the deflected angle measured by the autocollimator equipment is in excellent agreement with to that of measured by laser-based optical setup by using PSD. Therefore, both measurement methods are self-consistent. Conversely, one might say that the laser-based setup is as precise as the autocollimator method, since the Nikon autocollimator is a high precision equipment which can measure until 0.5’’ (second), i.e., 0.008’ (minute). Fig. 11(a) is the photograph of the finder view

taken when the mirror scanner is stopped and (b) when it is operating at the resonance frequency. The thick line in (a) is due to the curvature of the glass piece surface. This thickness has been removed in (b) so that only the residual image is remained. Since the scanner oscillation period (about 10ms) is higher than the camera shutter speed (67ms), the residual image appears on the photograph. This phenomenon is very convenient because it is possible to easily measure the deflected angle by the residual image thickness. Since our purpose was the verification of the device principle, the scanner has not been optimized for large deflection angle.

Finally, we have investigated the dependence relation between the deflected angle and the applied voltage as shown in Fig. 12 (a) and (b). For both graphs, the vertical axis is the PSD output voltage, which indirectly indicates the deflected angle. The horizontal axes are the applied peak-to-peak drive voltage in (a) and its square in (b). The latter shows a linear relation, and this is theoretically consistent, since the deflected angle is proportional to the square of the applied drive voltage.

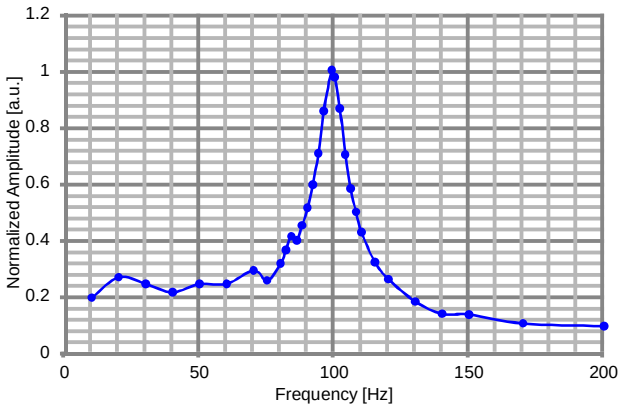

Figure 9 Frequency response (normalized)

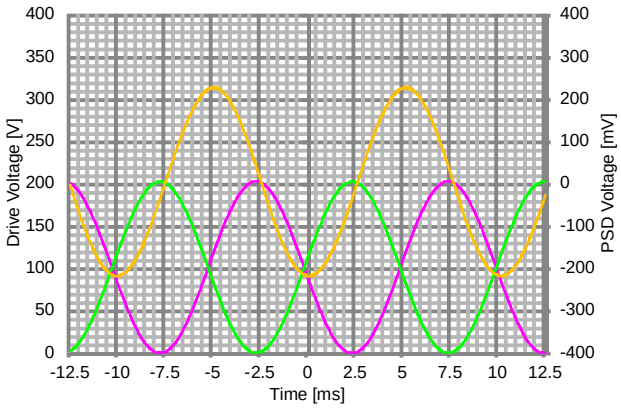

Figure 10 Voltage characteristics at resonance frequency

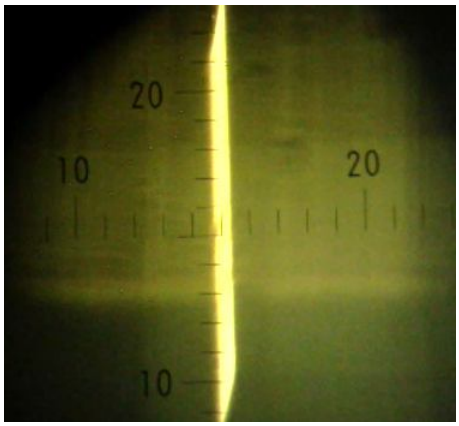

Figure 11 (a) Autocollimator image (scanner stopped)

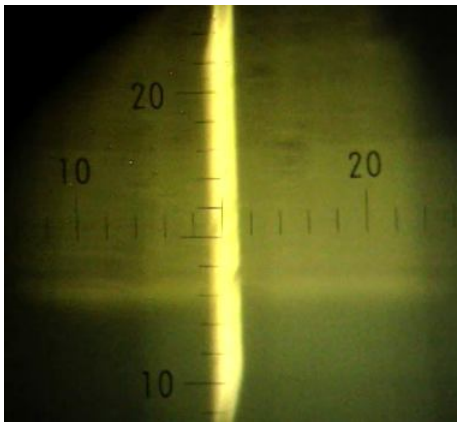

Figure 11 (b) Scanner under resonance operation

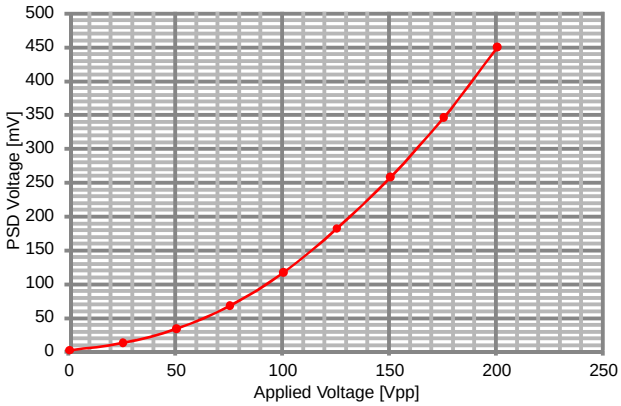

Figure 12 (a) PSD voltage (deflected angle) x applied voltage

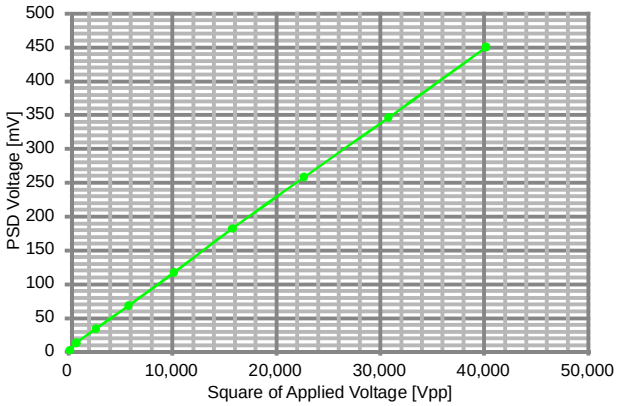

Figure 12 (b) Applied voltage has been squared

5.CONCLUSION

In this paper, we have designed, fabricated and characterized a SMEMS torsional mirror scanner, which has been fabricated by a stereolithography-based 3D-printer for the first time. We have obtained a frequency response similar to that of a mechanical resonator with a resonance frequency of 99Hz and a Q-factor of about 10. Thus, we demonstrated that the device performed a rotational motion, which is one of the important functions for electro-mechanical actuators. By using the same measurement setup, the maximum deflected angle was 1.12' (minute) at the resonance mode operation of the device. This value matched to that of measured by a high precision autocollimator. From this, it became clear that our laser-beam optical setup can also be used for high precision angle measurements. In addition, we have experimentally proved that electrostatically actuated comb-drives maintain a linear relation between the deflected angle and the square of the applied drive voltage.

At the moment, we are working on further development of the mirror scanner for larger deflection angle by means of reducing the comb fingers gap, optimizing the hinge structure and so on. The development of 3D printing technology are almost daily evolving, thus we are aiming to realize further miniaturization, high functionalization, and making high reliability of SMEMS devices

Acknowledgment

This work was supported by Ishinomaki Senshu University Research Grant.

REFERENCES

[1] C. Wu, Y. Xie, S. M. Mok, "Linking Product Design in CAD with Assembly Operations in CAM for Virtual Product Assembly," Assembly Automation, XXVII (4), pp. 309-323, 2007.

[2] G. Uzun, "An Overview of Dental CAD/CAM Systems," Biotechnology & Biotechnological Equipment," XXII (1), pp. 530-535, 2008.

[3] N. Prabhu, M. D. Anand, L. E. Ruban, "Structural Analysis of Scorbot-ER Vu Plus Industrial Robot Manipulator," Production & Manufacturing Research, II (1), pp. 309-325, 2014.

[4] D. A. Roberson, D. Espalin, R. B. Wicker, "3D Printer Selection: A Decision-Making Evaluation and Ranking Model," Virtual and Physical Prototyping, VIII (3), pp. 201-212, 2013.

[5] J. Mizuno, S. Takahashi, "A Fundamental Study of Sub-Millimeter Electro-Mechanical Systems (SMEMS) Structures," In Proceedings of the International Symposium on Fundamental and Applied Sciences 2014 (ISFAS 2014), pp. 1460-1462, 2014.

[6] J. Mizuno, S. Takahashi, "Characterization of an In-Plane Single-Sided Lateral Comb Actuator Fabricated by a 3D-Printer," The SIJ Transactions on Computer Science Engineering & its Applications, II (3), 2014.

[7] A. M. Hynes, H. Ashraf, J. K. Bhardwaj, J. Hopkins, I. Johnston, J. N. Shepherd, "Recent advances in silicon etching for MEMS using the ASETM Process," Sensor Actuator A: Physical, LXXIV (1-3), pp. 13-17, 1999.

[8] G. T. Mulhern, D. S. Soane, R. T. Howe, "Supercritical carbon dioxide drying of micro-structures," In Proceedings of the 7th International Conference on Solid-State Sensors, Actuators and Microsytems (Transducers '93), pp. 296-299, 1993.

[9] J. Mizuno, S. Takahashi, "Design and Fabrication of an Electrostatically Actuated Parallel-Plate Mirror by 3D-Printer," International Journal of Mechanical, Aerospace, Industrial and Mechatronics Engineering, VIII (3), 2014.

[10] J. Mizuno, S. Takahashi, "A Double-Sided In-Plane Lateral Comb-Drive Actuator Fabricated by a Plaster-Based 3D-Printer," In Proceedings of the International Conference on Machining, Materials and Mechanical Technologies (IC3MT 2014), 6pp, 2014.

[11] J. Mizuno, S. Takahashi, K. Suzuki, "Vertical Comb-Drive Actuated Torsional SMEMS Mirror Fabricated by a Plaster-Based 3D-Printer," In Proceedings of the International Congress on Natural Sciences and Engineering 2014 (ICNSE 2014), pp. 770-776, 2014.

AUTHORS

Dr. Eng. Jun Mizuno is an Associate Professor in the Department of Mechanical Engineering at Ishinomaki Senshu University (Japan). He received his Dr. Eng. Degree in 1999 and his M.E. Degree in 1996 from Tokyo Institute of Technology (Japan), and his B.E. Degree in 1994 from University of Sao Paulo (Brazil). His current research interests include Micro Electro-Mechanical Systems and Intelligent Robotics. He gives lectures on Control Engineering, Mechatronics, Robotics and Precision Machining. He is a member of Japanese Society of Applied Physics.

Takashi Kakizaki is currently working towards the Ms. Eng. Degree at the Department of Mechanical System Engineering at Ishinomaki Senshu University (Japan). He received his B.E. Degree in 2015 from the same University. His current research interests include Manufacturing of Micro Electro-Mechanical Actuators and Microfluidics based on 3D-Printers.

Dr. Eng. Satoshi Takahashi is an Associate Professor in the Department of Mechanical Engineering at Ishinomaki Senshu University (Japan). He received his Dr. Eng. Degree in 2011, his M.E. Degree in 2006, and his B.E. Degree in 2004 from Iwate University (Japan). His current research interests include Theoretical Analysis on Thermoelastic Problem in Thermal Barrier Coatings (TBCs), Functionally Graded Materials (FGMs), and Effective Practical Use of 3D-Printers. He gives lectures on Strength of Materials and Introduction to Computers. He is a member of The Japan Society of Mechanical Engineers, The Society of Material Science (Japan), Japan Society for Composite Materials, and Society of Automotive Engineers of Japan.

Dr. Eng. Subaru Kudo is a Professor in the Department of Information Technology and Electronics at Ishinomaki Senshu University (Japan). He received his Dr. Eng. Degree in 1995, his M.E. Degree in 1984 from Tohoku University (Japan), and his B.E. Degree in 1982 from Yamagata University (Japan). His current research interests include Ultrasonic Electronics. He gives lectures on Electric Circuit, Introduction to Electrical Signal Processing and Simulation Engineering. He is a member of The Acoustic Society of Japan.